Optimal State-Feedback Control of Bilinear DC-DC Converters with Guaranteed Regions of Stability

Carlos Olalla, *Member, IEEE*, Isabelle Queinnec,
Ramon Leyva, *Member, IEEE*, Abdelali El Aroudi, *Member, IEEE*

***Abstract*—This paper deals with the modeling and the robust controller synthesis for nonlinear dc-dc converters. In the first part of the paper, a model for the bilinear dynamics is presented. Such nonlinear dynamics can be included in a convex polytope such that the trajectories of the converter out of the equilibrium are assured to remain inside a guaranteed region of stability despite of the bilinear term. Such a description of the dynamic response of the converter is employed, in the second part of the article, to propose synthesis algorithms that can guarantee, a priori, the stability and performance requirements of the design. The resulting region of stability can take into account not only the bilinear terms but also the saturation of the control input, which is a topic of major importance in high-performance dc-dc converters. The aim of the paper is to contribute with a robust control framework which allows the designers to deal with the common requirements of regulated dc-dc converters. The correctness of the results has been verified both with numerical simulations and experimental measurements from dc-dc converter prototypes.**

I. Introduction

Switched mode dc-dc converters are the most popular devices to adapt voltage and current levels between dc sources and dc loads, since they maintain a low power loss in the conversion process [1]. Due to the inherent changes that usually appear in the power conversion system, as parametric uncertainty and current/voltage disturbances, dc-dc converters require a control subsystem to maintain the desired levels of current and/or voltage. Such a control subsystem must comply with several objectives: i) to assure the stability of the converter, ii) to fulfil the disturbance rejection requirements and iii) to satisfy the transient specifications of the system, which usually concern the settling time and overshoot of the regulated output.

Pulse-width modulation (PWM) is the most extended modulation method in dc-dc converters. Despite that there exist recent approaches that employ hybrid modeling [2], the power stage of the converter with PWM modulation is usually represented with an averaged model. Although such averaged models neglect the switched dynamics, they can take into account the inherent nonlinearities of the converter, as bilinear terms and saturations of the control input and the states. However, in conventional control approaches, these averaged models are linearized at an operating point in order to derive linear feedback laws, which are simpler and of lower cost than other nonlinear approaches. This approach may result in deteriorated output or undesired behavior, due to the uncertainty and the inherent nonlinearities of the converter.

The aforementioned characteristics of dc-dc converters and the requirements and limitations of the control subsystem have prompted several authors to seek for control methods which can deal appropriately with performance requirements, nonlinearities and parametric uncertainty, while maintaining low design and implementation costs. Recent examples of robust control synthesis for dc-dc converters are considered in [3]–[15]. Some of these papers propose nonlinear control laws as fuzzy-PID control [3], [4], active damping [5], model predictive control (MPC) [6], adaptive control [7], [8], variable structure control [9] and parameter-varying control laws [10], [11], but some of them do not consider explicitly the uncertainty or the nonlinearities of the converter [3]–[5] and others result in nonlinear or time-varying control laws which are complex to implement [3]–[11]. On the other hand, linear control laws of the same difficulty degree that those used by practitioners are shown in [12]–[15]. The $\mathcal{H}_\infty$ method is treated in [12], while a design based on quantitative feedback theory (QFT) is deployed in [13]. Finally, [14], [15] proposed robust control approaches based on linear matrix inequalities (LMIs) and optimization methods.

This work is concerned with the investigation of control synthesis methods that result in simple implementations, and concretely with the investigation of LMI control for dc-dc converters, since it presents several advantages. In the first place, the LMI formulation of the synthesis problem can include several design requirements and optimization criteria, as for example: an $\mathcal{H}_\infty$ disturbance rejection bound [16], pole placement restrictions [17] and control effort constraints [18]. Besides, the synthesis procedure can cope with the uncertainty and the nonlinearities of the converter while maintaining the simplicity of the control problem formulation [19]. Finally, the solution of the state-feedback problem in LMI formulation can be solved by means of very efficient convex optimization algorithms [20] that allow to obtain the optimal controller [21] while maintaining the simplicity of the control law. This ap-

C. Olalla is a visiting scholar in the Colorado Power Electronics Center (CoPEC), Department of Electrical, Computer, and Energy Engineering, University of Colorado, Boulder CO, USA.

C. Olalla, R. Leyva and A. El Aroudi are with the Departament d'Enginyeria Electrònica, Elèctrica i Automàtica, Escola Tècnica Superior d'Enginyeria, Universitat Rovira i Virgili, 43007, Tarragona, Spain (e-mail:com.ea@tinet.org).

I. Queinnec is with CNRS ; LAAS ; 7 avenue du Colonel Roche, F-31077 Toulouse, France and Université de Toulouse ; UPS , INSA , INP, ISAE ; LAAS ; F-31077 Toulouse, France.

proach results in large signal stability and tight performances.

The synthesis method that is proposed in this paper deals with the following aspects. It considers the usual specifications of dc-dc converters concerning transient characteristics and disturbance rejection specifications, as in [14], [15]. The parametric uncertainty of the converter and the different operating points are also taken into account, with an improved version of the polytope shown in those papers [14], [15]. Besides, the proposed synthesis method allows to guarantee a region of stability, so that the trajectory between different operation points is assured to be stable despite the bilinear term, which is a major improvement with respect to previous works. Another contribution of the paper is that the region of stability is completely guaranteed by taking into account the saturation nonlinearity of the control input. Finally, the proposed time-invariant control law maintains the low implementation cost if compared with the linear parameter-variant controllers shown in [10], [11]. The last contribution of this paper is the proposed implementation circuit, which allows to realize the state-feedback loop with a reduced number of operational amplifiers and discrete elements. The experimental results corroborate the analytical derivations presented in the paper.

The rest of the paper is outlined as follows. Section II describes the modeling of a dc-dc converter which allows to take into account the uncertainty and the bilinear dynamics. In Section III, the conditions for robust performance and robust stability are expressed as LMIs. Section IV presents synthesis algorithms that take into account the performances, uncertainties and nonlinearities of the dc-dc converter. First, an analysis algorithm that allows to obtain the region of stability for a given controller is introduced. Then, a synthesis algorithm which can deal with the trade-off between performance and stability is presented. Such a synthesis algorithm is employed to design a robust controller for a boost converter in Section V. An experimental set up of the design example is deployed in Section VI, where the validity of this design procedure is demonstrated and where this approach is compared with the method shown in [15], in order to illustrate its advantages. Section VII summarizes the key aspects of this paper and presents some conclusions and perspectives.

II. Modeling of Bilinear Power Converters

This section deals with the modeling of uncertainties and nonlinearities in dc-dc converters. The approach shown here is related to the step-up (boost) converter, but it can be easily adapted for other bilinear converters.

A. Averaged Model of a PWM Boost Converter

Fig. 1 shows the circuit diagram of a dc-dc boost converter where $v_{\rm o}(t)$ is the output voltage, $v_{\rm g}(t)$ is the line voltage and $i_{\rm load}(t)$ is the load disturbance. The output voltage must be kept at a given value $v_{\rm ref}(t)$. The converter load is modeled as a linear resistor R. The capacitance of the capacitor and the inductance of the inductor are represented, respectively, by C and L. Their equivalent series resistances, r_C and r_L, are considered sufficiently small to be neglected. Thus, the measurable states of the converter are the inductor current

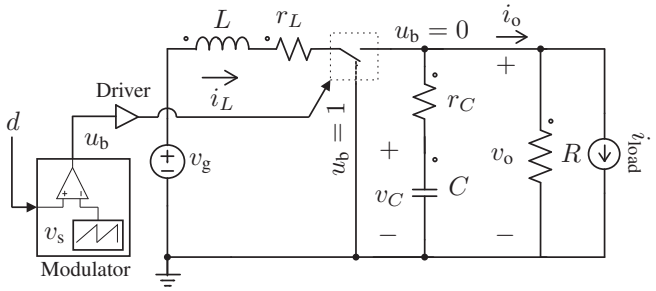

Figure 1. Schematic of the boost converter.

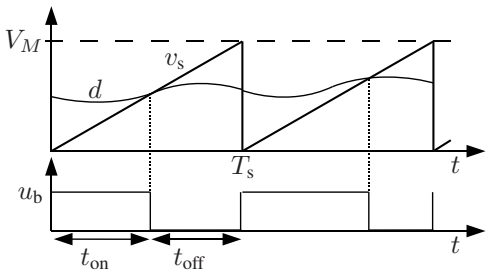

Figure 2. Waveforms of the PWM process.

$i_L(t)$ and the capacitor voltage $v_C(t)=v_{\rm o}(t)$. Note that the time dependence of the variables may be omitted to simplify the notation.

The binary signal $u_{\rm b}(t)$, which turns on and off the switches, is controlled by means of a fixed-frequency PWM (see Fig. 2). The constant switching frequency is $1/T_{\rm s}$, where $T_{\rm s}$ is the switching period equal to the sum of $t_{\rm on}$ and $t_{\rm off}$. The ratio $t_{\rm on}/T_{\rm s}$ is defined as the duty-cycle of the converter, noted $d(t)$. If the duty-cycle is compared with a sawtooth voltage signal $v_{\rm s}(t)$ of amplitude $V_M=1$ V, then the control input is not saturated for $0\leq d(t)\leq 1$. It is assumed that the converter operates in the continuous conduction mode (CCM) and that the inductor current is not saturated.

The state-space averaged model of a dc-dc converter, as described in [22], can be written as:

$$\begin{aligned}\dot{\tilde{x}}_{\rm a} = {} & \big(A_{\rm off}+(A_{\rm on}-A_{\rm off})U\big)X_{\rm a}+\ldots\\ & \big(B_{\rm off}+(B_{\rm on}-B_{\rm off})U\big)\left[\begin{smallmatrix}1\\0\end{smallmatrix}\right]W\\ & +\big(A_{\rm off}+(A_{\rm on}-A_{\rm off})U\big)\tilde{x}_{\rm a}+\ldots\\ & \big(B_{\rm off}+(B_{\rm on}-B_{\rm off})U\big)\left[\begin{smallmatrix}0\\1\end{smallmatrix}\right]\tilde{w}\\ & +\big((A_{\rm on}-A_{\rm off})X_{\rm a}+(B_{\rm on}-B_{\rm off})\left[\begin{smallmatrix}1\\0\end{smallmatrix}\right]W\big)\tilde{u}\\ & +\big((A_{\rm on}-A_{\rm off})\tilde{x}_{\rm a}+(B_{\rm on}-B_{\rm off})\left[\begin{smallmatrix}0\\1\end{smallmatrix}\right]\tilde{w}\big)\tilde{u},\end{aligned} \tag{1}$$

where $A_{\rm on}$ and $B_{\rm on}$ are the state-space matrices during $t_{\rm on}$ and $A_{\rm off}$ and $B_{\rm off}$ are the state-space matrices during $t_{\rm off}$. The incremental and equilibrium input vectors are $\tilde{u}(t)$ and U, while the incremental and equilibrium state vectors are $\tilde{x}_{\rm a}(t)$ and $X_{\rm a}$, respectively. In addition, the incremental and steady-state vector of disturbance inputs, which corresponds to the output current disturbance $i_{\rm load}(t)$ and the input voltage $V_{\rm g}$, are noted as $\tilde{w}(t)$ and W. In the boost converter, these vectors

are written as follows:

$$U = D, \qquad X_{\rm a} = \begin{bmatrix} \frac{V_g}{D'^2 R} \\ \frac{V_g}{D'} \end{bmatrix}, \qquad W = V_{\rm g}, \tag{2}$$
$$\tilde{u}(t) = \tilde{d}(t), \quad \tilde{x}_{\rm a}(t) = \begin{bmatrix} \tilde{i}_L(t) \\ \tilde{v}_{\rm o}(t) \end{bmatrix}, \quad \tilde{w}(t) = \tilde{i}_{\rm load}(t).$$

In order to obtain zero steady-state error between the constant voltage reference $V_{\rm ref}$ and the output voltage $v_o(t)$, the model is augmented with an additional state variable $x_{\rm int}(t)$, which stands for the integral of the output voltage error, i.e. $x_{\rm int}(t) = -\int \big(V_{\rm ref} - v_{\rm o}(t)\big) dt$. Also, an error coordinates representation is introduced as in [23]. Considering that the error state is $e(t) = v_{\rm o}(t) - V_{\rm ref}$, the state vector of the new model is then written as:

$$x(t) = \begin{bmatrix} i_L(t) \\ e(t) \\ x_{\rm int}(t) \end{bmatrix} = \begin{bmatrix} i_L(t) \\ v_{\rm o}(t) \\ x_{\rm int}(t) \end{bmatrix} - \begin{bmatrix} 0 \\ 1 \\ 0 \end{bmatrix} V_{\rm ref}. \tag{3}$$

Since the steady-state part is $AX + B_W W = 0$, the averaged model of (1) can then be written as:

$$\begin{gathered} \dot{\tilde{x}}(t) = A\tilde{x}(t) + B_{\tilde{w}}\tilde{w}(t) + B_u\tilde{u}(t) + B_{\rm n}\tilde{x}(t)\tilde{u}(t), \\ A = \begin{bmatrix} 0 & -\frac{D'}{L} & 0 \\ \frac{D'}{C} & -\frac{1}{RC} & 0 \\ 0 & 1 & 0 \end{bmatrix}, \; B_u = \begin{bmatrix} \frac{V_{\rm g}}{D'L} \\ -\frac{V_{\rm g}}{D'^2 RC} \\ 0 \end{bmatrix}, \\ B_{\tilde{w}} = \begin{bmatrix} 0 \\ -\frac{1}{C} \\ 0 \end{bmatrix}, \; B_{\rm n} = \begin{bmatrix} 0 & \frac{1}{L} & 0 \\ -\frac{1}{C} & 0 & 0 \\ 0 & 0 & 0 \end{bmatrix}, \end{gathered} \tag{4}$$

where $D' = 1 - D$ is the complementary steady-state duty-cycle. This model involves a linear part $A\tilde{x}(t) + B_{\rm u}\tilde{u}(t) + B_{\tilde{w}}\tilde{w}(t)$ and a bilinear part $B_{\rm n}\tilde{x}(t)\tilde{u}(t)$. The dimensions of the system matrices are defined as A, $B_{\rm n} \in \mathbb{R}^{n\times n}$, $B_u \in \mathbb{R}^{n\times m}$ and $B_{\tilde{w}} \in \mathbb{R}^{n\times l}$, where $n = 3$, $m = 1$ and $l = 1$.

B. Polytopic Model of Uncertainties

In order to deal with the converter uncertainty, let us first consider the linear part of the averaged model, obtained when the bilinear term is neglected. In the boost converter, it is considered that the load R and the complementary duty-cycle at the operating point D' are the most relevant uncertain terms:

$$D' \in [0.3,\ 1], \quad \frac{1}{R} \in \left[\frac{1}{50},\ \frac{1}{10}\right]. \tag{5}$$

Matrices A and B_u depend on these parameters, but non-linearly. To account for a convex polytopic description of the uncertainty, each nonlinear block has to be considered independently of the parameters which compose it. This set of parameters can then be coupled in a vector $p = \big(p_1, \ldots, p_{n_p}\big)$.

Therefore, the linear part of the averaged model of the converter, with no external inputs, can be written as:

$$\dot{\tilde{x}}(t) = A(p)\tilde{x}(t) + B_u(p)\tilde{u}(t) \tag{6}$$

Such uncertain matrices $A(p), B_u(p)$ can be included in a convex polytope, defined by its vertices $\{\mathcal{G}_1, \ldots, \mathcal{G}_N\}$:

$$\begin{gathered} [A(p), B_u(p)] \in \text{Co}\,\{\mathcal{G}_1, \ldots, \mathcal{G}_N\} := \\ \left\{\sum_{i=1}^N \lambda_i \mathcal{G}_i, \quad \lambda_i \geq 0, \quad \sum_{i=1}^N \lambda_i = 1\right\}. \end{gathered} \tag{7}$$

Table I
VERTICES OF THE POLYTOPE OF UNCERTAINTY.

Vertex #	D'	$1/D'$	$1/(D'^2 R)$	$1/R$
$\rm v_1$	0.3	3.3	$11.1 \cdot (1/10)$	1/10
$\rm v_2$	0.3	3.3	$11.1 \cdot (1/50)$	1/50
$\rm v_3$	0.425	1.6	$2.25 \cdot (1/10)$	1/10
$\rm v_4$	0.425	1.6	$2.25 \cdot (1/50)$	1/50
$\rm v_5$	0.425	2	$2.25 \cdot (1/10)$	1/10
$\rm v_6$	0.425	2	$2.25 \cdot (1/50)$	1/50
$\rm v_7$	1	1	$1 \cdot 1/10$	1/10
$\rm v_8$	1	1	$1 \cdot 1/50$	1/50

For the boost converter, an uncertainty vector of 4 parameters is proposed: $p = [D',\ 1/D',\ 1/(D'^2 R),\ 1/R]$. With a classical polytopic approach, such an uncertainty vector would result in 2^4 vertices, which are reduced in the current case to $N = 8$ vertices given in Table I, thanks to an adequate polytopic covering (examples in [24]). Such a polytope is therefore formed with the following system matrices:

$$\begin{gathered} [A(p), B_u(p)] \in \mathcal{P}_{\rm new} = \text{Co}\,\{\mathcal{G}_1, \ldots, \mathcal{G}_N\} : \\ \begin{array}{ll} \mathcal{G}_1 = [A(\rm v_1),\ B_u(\rm v_1)], & \mathcal{G}_2 = [A(\rm v_2),\ B_u(\rm v_2)], \\ \mathcal{G}_3 = [A(\rm v_3),\ B_u(\rm v_3)], & \mathcal{G}_4 = [A(\rm v_4),\ B_u(\rm v_4)], \\ \mathcal{G}_5 = [A(\rm v_5),\ B_u(\rm v_5)], & \mathcal{G}_6 = [A(\rm v_6),\ B_u(\rm v_6)], \\ \mathcal{G}_7 = [A(\rm v_7),\ B_u(\rm v_7)], & \mathcal{G}_8 = [A(\rm v_8),\ B_u(\rm v_8)]. \end{array} \end{gathered} \tag{8}$$

With this polytope, the converter will be assured to remain stable for the set of loads and operating points expressed in the uncertainty description of (5).

Note that for a constant output voltage (which is the case considered in the paper), a change in the operating point duty-cycle implies a change in V_g, i.e. the uncertainty of V_g that is contained in the model is $V_g \in [V_o \cdot \underline{D'}, V_o \cdot \overline{D'}]$.

C. Polytopic Model of Bilinear Dynamics

The bilinear part of the dynamics, which is usually overlooked, can destabilize the closed-loop converter out of the considered operating point. In other words, different equilibrium points can be expressed with the uncertainty model of the previous subsection, however there is no proof of stable trajectory between these points. The representation of the uncertain converter in such a equilibrium point is as follows:

$$\dot{\tilde{x}}(t) = A\tilde{x}(t) + B_{\rm u}\tilde{u}(t) + B_{\rm w}\tilde{w}(t) + B_{\rm n}\tilde{x}(t)\tilde{u}(t). \tag{9}$$

The polytopic modeling of bilinear terms presented in [25] has been adapted to the converter model in order to cope with the effect of such bilinear terms on the stability of the closed-loop system. With this method, the possible values of the term $B_{\rm n}\tilde{x}(t)$ are included in a convex polytope $\mathcal{X}(\tilde{x})$:

$$\mathcal{X}(\tilde{x}) = \text{Co}\{v_j, j = 1, \ldots, N_b\}. \tag{10}$$

where $N_b = 2^n$ is the number of vertices of $\mathcal{X}(\tilde{x})$. Note that the same procedure can be applied to represent the possible values of $B_{\rm n}\tilde{u}(t)$, but in our case the representation of $B_{\rm n}\tilde{x}(t)$ yielded better results. In a general case, for any $\tilde{x} \in \mathcal{X}(\tilde{x})$,

one has

$$\begin{aligned}[B_{\mathrm{n}_1}\tilde{x}(t)\ \ldots\ B_{\mathrm{n}_m}\tilde{x}(t)] &= \sum_{j=1}^{N_b}\beta_j\,[B_{\mathrm{n}_1}v_j\ \ldots\ B_{\mathrm{n}_m}v_j] \\ &= \sum_{j=1}^{N_b}\beta_j\mathbb{B}_j = \mathbb{B}(\beta)\end{aligned} \tag{11}$$

with $\beta_j \in \mathbb{R}^{N_b}$ belonging to the convex set

$$\mathcal{U} = \left\{\beta \in \mathbb{R}^{N_b}; \sum_{j=1}^{N_b}\beta_j = 1, \beta_j \geq 0, j = 1,\ldots,N_b\right\} \tag{12}$$

The possible values of the vertices of $\mathcal{X}(\tilde{x})$ are set up in a symmetric space as $\mathcal{X}(\tilde{x}) = \{\tilde{x} \in \mathbb{R}^n; -\mu \leq \tilde{x} \leq \mu\}$, where $\mu \in \mathbb{R}^n$ represents a set of possible variations of the state vector. Thus, vertices v_j are obtained from μ by the linear combination

$$v_j = \Delta_j\mu,\ j = 1,\ldots,N_b, \tag{13}$$

where Δ_j are diagonal matrices formed with the possible combinations of ± 1.

In the specific case of the boost converter (9), there exists only one bilinear term $B_{\mathrm{n}_1} = B_{\mathrm{n}}$ which is modeled for the possible values of $\tilde{x}(t)$ in $\mathcal{X}(\tilde{x})$ as $\mathbb{B}(\beta)$. Thus, the converter dynamics can be written as:

$$\dot{\tilde{x}}(t) = A\tilde{x}(t) + \big(B_u + \mathbb{B}(\beta)\big)\tilde{u}(t) + B_{\mathrm{w}}\tilde{w}(t) \tag{14}$$

In this case, it is worth to point out that the third column of matrix B_{n} is zero, which in practice means that the state x_{int} does not affect the bilinear dynamics of the boost converter. Consequently, the vertices v_j do not require to consider the third state of the converter, i.e. they are obtained with $N_b = 2^{(n-1)} = 4$ diagonal matrices Δ_j as follows

$$\Delta_j = \begin{bmatrix}\pm 1 & 0 & 0\\ 0 & \pm 1 & 0\\ 0 & 0 & 0\end{bmatrix}. \tag{15}$$

Therefore, in the boost converter, for a bound on the states $\mu = [\tilde{i}_{\mathrm{L}_0},\ \tilde{v}_{\mathrm{C}_0},\ \tilde{x}_{\mathrm{int}_0}]'$, vertices v_j would be defined as:

$$\begin{aligned} v_1 &= \begin{bmatrix}\tilde{i}_{\mathrm{L}_0} & \tilde{v}_{\mathrm{C}_0} & 0\end{bmatrix}' & v_2 &= \begin{bmatrix}-\tilde{i}_{\mathrm{L}_0} & \tilde{v}_{\mathrm{C}_0} & 0\end{bmatrix}' \\ v_3 &= \begin{bmatrix}\tilde{i}_{\mathrm{L}_0} & -\tilde{v}_{\mathrm{C}_0} & 0\end{bmatrix}' & v_4 &= \begin{bmatrix}-\tilde{i}_{\mathrm{L}_0} & -\tilde{v}_{\mathrm{C}_0} & 0\end{bmatrix}'\end{aligned} \tag{16}$$

III. LMI Conditions for Stability and Performance

This section proposes LMI conditions to derive an optimal control law for the robust control of a boost converter. Considering the control scheme depicted in Fig. 3, the closed-loop scheme consists of a state-feedback controller $\mathbf{K}$, such that the control input is equal to:

$$\tilde{u} = \mathbf{K}\tilde{x} = K_1\cdot\tilde{i}_{\mathrm{L}} + K_2\cdot\tilde{v}_{\mathrm{C}} + K_3\cdot\tilde{x}_3. \tag{17}$$

The ripple propagated in $\tilde{u}$ is considered small enough to avoid chaotic behavior.

The first part of the section presents the LMI conditions that assure the closed-loop performance while the second part introduces the constraints that guarantee the stability of the converter despite the nonlinearities, as the bilinear terms and the saturation of the duty-cycle. Each LMI condition is briefly discussed. For detailed proofs of each constraint, see the mentioned references.

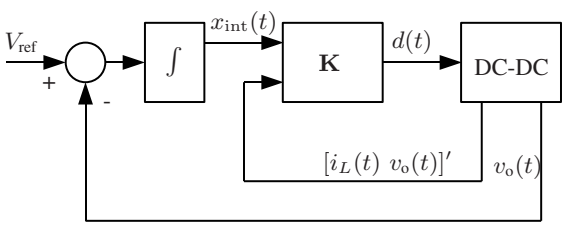

Figure 3. Block diagram of a linear state-feedback system.

A. Performance Constraints

With the LMI $\mathcal{H}_\infty$ control method [26] method, the designer can obtain the control gain $\mathbf{K}$ that guarantees the optimal $\mathcal{H}_\infty$ norm between the disturbance input i_{load} and the regulated output v_{o}, assuring a minimum disturbance rejection level λ. Besides, several transient performances, as for example, the decay rate and overshoot of the output voltage are also guaranteed. Such transient performances, which are of critical interest in dc-dc converters, are specified by a set of constraints [16], [17], which assure the location of the closed-loop poles in the region $\mathcal{S}(\alpha,\ \theta,\ \rho)$. This region, for the (complex) poles of the system in the form $x \pm jy$, corresponds to:

$$x < -\alpha < 0, \quad y < \cot(\theta)x, \quad |x \pm jy| < \rho \tag{18}$$

These performances are considered in the vicinity of the operating points of the converter and consequently the bilinear term is not taken into account.

Proposition 1. *The uncertain system* (9)*, where the bilinear term is neglected, with the output vector* $\tilde{y}(t) = C_x\tilde{x}(t) + D_u\tilde{u}(t)$*, is stabilizable by state-feedback* $\tilde{u} = \mathbf{K}\tilde{x}$*, with* $\mathcal{H}_\infty$ *norm* ($\sup\frac{\|y(t)\|_2}{\|w(t)\|_2}$) *lower than* λ *and with the closed-loop poles inside the region* $\mathcal{S}(\alpha,\ \theta,\ \rho)$*, if and only if there exist a symmetric definite positive matrix* $\mathbf{W} \in \mathbb{R}^{n\times n}$ *and a matrix* $\mathbf{Y} \in \mathbb{R}^{m\times n}$ *such that the following inequalities hold:*

$$\begin{bmatrix} A_i\mathbf{W} + \mathbf{W}A_i' + B_{u_i}\mathbf{Y} + \mathbf{Y}'B_{u_i}' & B_{\tilde{w}} & \mathbf{W}C_x' + \mathbf{Y}'D_u' \\ B_{\tilde{w}}' & -\lambda\mathbb{1} & 0 \\ C_x\mathbf{W} + D_u\mathbf{Y} & 0 & -\lambda\mathbb{1}\end{bmatrix} < 0 \tag{19}$$

$$A_i\mathbf{W} + \mathbf{W}A_i' + B_{u_i}\mathbf{Y} + \mathbf{Y}'B_{u_i}' + 2\alpha\mathbf{W} < 0 \tag{20}$$

$$\begin{bmatrix} \cos\theta(A_i\mathbf{W} + \mathbf{W}A_i' + B_{u_i}\mathbf{Y} + \mathbf{Y}'B_{u_i}') & \\ \sin\theta(-A_i\mathbf{W} + \mathbf{W}A_i' - B_{u_i}\mathbf{Y} + \mathbf{Y}'B_{u_i}') & \\ \cos\theta(A_i\mathbf{W} + \mathbf{W}A_i' + B_{u_i}\mathbf{Y} + \mathbf{Y}'B_{u_i}') & \\ \sin\theta(A_i\mathbf{W} - \mathbf{W}A_i' + B_{u_i}\mathbf{Y} - \mathbf{Y}'B_{u_i}') & \end{bmatrix} < 0 \tag{21}$$

$$\begin{bmatrix} -\rho\mathbf{W} & \mathbf{W}A_i' + \mathbf{Y}'B_{u_i}' \\ A_i\mathbf{W} + B_{u_i}\mathbf{Y} & -\rho\mathbf{W}\end{bmatrix} < 0 \tag{22}$$

For all vertices of the uncertainty model: $\forall i = 1,\ldots,N$*. The controller is recovered by* $\mathbf{K} = \mathbf{Y}\mathbf{W}^{-1}$.

The disturbance rejection bound is complied if inequality (19) holds, while the poles are placed in the region $\mathcal{S}(\alpha,\ \theta,\ \rho)$ if inequalities (20), (21), (22) are verified.

B. Stability Constraints

In a linear system, the region of stability is the whole state space $\mathbb{R}^n$. However, if the bilinearity of the system is taken into account, the region of attraction may be only local, and it is necessary to estimate this region of stability of the system out of the operating point (its exact characterization is in general a complex task).

We consider an approximation of the region of stability, noted ε, which is defined by a quadratic Lyapunov function $V(\tilde{x}) = \tilde{x}'\mathbf{P}\tilde{x}$ to assure the stability of the boost converter as expressed in (9). The conditions of stability are then based on the classic concepts of Lyapunov theory [19]. These conditions have been addressed in [25] through the following proposition, in which $\mathbf{W} = \mathbf{P}^{-1}$.

Proposition 2. *The bilinear system* (9)*, where* $\tilde{w}(t) = 0$*, is stabilizable by state-feedback* $\tilde{u} = \mathbf{K}\tilde{x}$*, with a guaranteed region of stability* $\varepsilon(\mathbf{P}, 1)$ *if and only if there exist a symmetric definite positive matrix* $\mathbf{W} \in \mathbb{R}^{n\times n}$ *and a matrix* $\mathbf{Y} \in \mathbb{R}^{m\times n}$ *such that the following inequalities hold:*

$$[A_k\mathbf{W} + \mathbf{W}A_k' + (B_{u_k} + [B_{\mathrm{n}}\Delta_j\mu])\mathbf{Y} + \mathbf{Y}'(B_{u_k} + [B_{\mathrm{n}}\Delta_j\mu])'] < 0 \tag{23}$$

$$\begin{bmatrix} \mu_{(r)}\mathbf{W} & \mathbf{W}\mathbb{1}_{(r)}' \\ \mathbb{1}_{(r)}\mathbf{W} & \mu_{(r)} \end{bmatrix} \geq 0 \tag{24}$$

For all vertices of the uncertainty model: $\forall k = 1, \ldots, N_k$*, for all vertices of the bilinearity model:* $\forall j = 1, \ldots, N_b$ *and for all states of the converter:* $\forall r = 1, \ldots, n$*. The controller is recovered by* $\mathbf{K} = \mathbf{Y}\mathbf{W}^{-1}$.

The quadratic Lyapunov function $V(\tilde{x}) = \tilde{x}'\mathbf{P}\tilde{x} = \tilde{x}'\mathbf{W}^{-1}\tilde{x}$ defines an ellipsoid in $\mathbb{R}^n$:

$$\varepsilon(\mathbf{P}, 1) := \{\tilde{x} \in \mathbb{R}^n; \tilde{x}'\mathbf{W}^{-1}\tilde{x} \leq 1\} \tag{25}$$

which corresponds to the assured region of stability of the system. By inequality (24), this ellipsoid is included in the polyhedral region of the bilinear model, i.e. $\varepsilon(\mathbf{P}, 1) \subseteq \mathcal{X}(\tilde{x})$. Since inequality (23) assures that $\dot{V}(\tilde{x})$ is strictly negative inside $\mathcal{X}(\tilde{x})$, the trajectories of the system that belong to $\varepsilon(\mathbf{P}, 1)$ will remain inside this contractive region despite the bilinear term.

C. Control Effort Constraint

In order to avoid the saturation of the duty-cycle, the following constraint, also adapted from [25], is used to limit the incremental control input to $-u_0 \leq \mathbf{K}\tilde{x} \leq u_0$ with the following LMI:

$$\begin{bmatrix} \mathbf{W} & \mathbf{Y}' \\ \mathbf{Y} & u_0^2 \end{bmatrix} \geq 0. \tag{26}$$

Given that $\mathbf{K} = \mathbf{Y}\mathbf{W}^{-1}$. With this LMI, the region of stability $\varepsilon(\mathbf{P}, 1)$ is included in the set $u_0^2 \geq \tilde{x}'\mathbf{K}'\mathbf{K}\tilde{x}$. Note that this last requirement only makes sense for a certain operating point.

Remark III.1. *For a given controller* $\mathbf{K}$*, inequalities* (19)-(26) *can be transformed easily with congruence transformations to analyse the region of stability of the system. The resulting LMI conditions are noted* $(19)^*$-$(26)^*$.

IV. Proposed Optimal Control Synthesis Methods

The previous LMI conditions are used in this section to propose the following analysis and synthesis procedures. They can be easily coded with standard tools such as MATLAB [20].

A. Analysis of the Guaranteed Region of Stability

Given a state-feedback controller $\mathbf{K}$, the largest region of stability despite the bilinear term, in which the duty cycle remains nonsaturated, can be found with Algorithm 1. In this algorithm, the choice of the state-vector μ determines the size of the stability region $\varepsilon(\mathbf{P}, 1)$, since $\varepsilon(\mathbf{P}, 1) \subseteq \mathcal{X}(\tilde{x})$. In order to cope with this limitation, the synthesis algorithm for the enlargement of $\mathcal{X}(\tilde{x})$ consists on fixing μ while searching for the rest of variables $\mathbf{W}, \mathbf{Y}$ and then to take the results of these variables to enlarge μ as much as possible.

Analysis Algorithm 1.
Step 1: Initialization. Given a controller $\mathbf{K}$*, choose an initial* μ *sufficiently small and define* u_0.
Step 2: Compute $\mathbf{P}$ *solution to:*

$$\begin{aligned} \min_{\mathbf{P}} \ & \mathrm{Tr}(\mathbf{P}) \ \text{ subject to} \\ & \text{LMIs } (23)^*, (24)^* \text{ and } (26)^*. \end{aligned} \tag{27}$$

Step 3: Fix $\mathbf{P}$*. Compute* $\mu_{(r)},\ r = 1, \ldots, n$ *solution to:*

$$\max \ \sum_{r=1}^{n} \mu_{(r)} \ \text{ subject to } \ \text{LMI } (24)^*. \tag{28}$$

Step 4: Return to Step 2 until the reduction of ($\mathrm{Tr}(\mathbf{P})$*) is not large enough.*
Step 5: The region of stability with controller $\mathbf{K}$ *is given by* $\varepsilon(\mathbf{P}, 1)$.

B. Synthesis with a Guaranteed Level of Performance

The analysis of a given controller can be useful to verify the stability of the nonlinear converter. However, this paper is focused on proposing new synthesis methods. If the designer has some performance requirements that must be fulfilled, as the settling time, the maximum overshoot, the minimum disturbance rejection ratio and the maximum affordable control effort, Algorithm 1 can be used to derive a controller $\mathbf{K}$ with the largest possible region of stability for those requirements.

Synthesis Algorithm 1.
Step 1: Initialization. Choose $\alpha,\ \rho,\ \theta,\ \lambda,\ u_0,\ \mu$.
Step 2: Compute $\mathbf{W}, \mathbf{Y}$ *solution to:*

$$\begin{aligned} \min_{\mathbf{W},\mathbf{Y}} \ & \mathrm{Tr}(\mathbf{T}) \ \text{ subject to} \\ & \text{LMIs } (19), (20), (21), (22), (23), (24), (26) \text{ and} \\ & \begin{bmatrix} \mathbf{T} & \mathbb{1} \\ \mathbb{1} & \mathbf{W} \end{bmatrix} \geq 0 \end{aligned} \tag{29}$$

Step 3: Fix $\mathbf{W}, \mathbf{Y}$*. Compute* $\mu_{(r)},\ r = 1, \ldots, n$ *solution to:*

$$\max \ \sum_{r=1}^{n} \mu_{(r)} \ \text{ subject to } \ \text{LMI } (24). \tag{30}$$

Step 4: Return to Step 1 until the reduction of $\mathrm{Tr}(\mathbf{T})$ *is not large enough.*

Step 5: The controller is recovered by $\mathbf{K} = \mathbf{Y}\mathbf{W}^{-1}$. *The region of stability despite the bilinear term is given by* $\varepsilon(\mathbf{P}, 1)$

C. Synthesis with Optimal Performance

Since designers must usually have to deal also with a required region of stability, an improvement of the previous Algorithm 1 is proposed. In the following synthesis algorithm, the objective is to find the smallest possible $\mathcal{H}_\infty$ norm (λ) from disturbance to output, while assuring that the region of stability is large enough to contain the trajectories of the converter between specific operation points x_{0_k} given beforehand. Such a condition is fulfilled if the following LMI holds:

$$\begin{bmatrix} \mathbb{1} & x_{0_k} \\ x_{0_k} & \mathbf{W} \end{bmatrix} > 0 \tag{31}$$

Since the optimization of the $\mathcal{H}_\infty$ performance can result in a very small region of attraction, the inclusion of x_{0_k} in the region of stability allows to maintain the robustness while achieving the best possible performance.

The initial choice of μ must be large enough so that $\varepsilon(\mathbf{P}, 1)$ can contain x_{0_k}, but small enough so that the performance requirements can be achieved. If the system is stable in open-loop, it can be assured that a sufficiently large μ can always be found, at the expense of lower performances.

Synthesis Algorithm 2.
Step 1: Initialization. Choose $\alpha,\ \rho,\ \theta,\ u_0$. *Choose* μ *large enough so that* $\varepsilon(\mathbf{P}, 1)$ *can contain the points* x_{0_k}, *but small enough so that the performance and the control effort constraints are feasible.*
Step 2: Compute $\mathbf{W}, \mathbf{Y}, \lambda$ *solutions to:*

$$\min_{\mathbf{W},\mathbf{Y}} \ \lambda \ \text{ subject to}$$
$$\text{LMIs (19), (20), (21), (22), (23), (24), (31) and (26).}$$

Step 3: Fix $\mathbf{W}, \mathbf{Y}$. *Compute* $\mu_{(r)},\ r = 1, \ldots, n$ *solution to:*

$$\min \ \sum_{r=1}^{n} \mu_{(r)} \ \text{ subject to } \ \text{LMI (24).}$$

Step 4: Return to Step 1 until the reduction of λ *is not significative.*
Step 5: The controller is recovered by $\mathbf{K} = \mathbf{Y}\mathbf{W}^{-1}$ *and the minimum disturbance rejection for such a controller is given by* λ. *The region of stability for this performance is* $\varepsilon(\mathbf{P}, 1)$.

This algorithm provides a compact framework to deal with the performance requirements, the uncertainty and the nonlinearities of the converter. However, sometimes it may be difficult to find a region $\varepsilon(\mathbf{P}, 1)$ that satisfies the performance requirements and the control effort constraints at the same time. Consequently, the final algorithm that is proposed in this paper combines the synthesis capabilities of Synthesis Algorithm 2 with Analysis Algorithm 1.

D. Synthesis with Optimal Performance and Analysis of Control Effort

This algorithm allows to synthesize a controller that assures the performance and robustness constraints in two steps. A controller is synthesized first without the control effort constraint. Then, the closed-loop system with the derived controller is analyzed and the control effort constraint is verified to hold. This approach allows to obtain the needed degree of freedom in the optimization program to achieve tight performances and robust stability.

Synthesis Algorithm 3.
Step 1: Initialization. Choose $\alpha,\ \rho,\ \theta$. *Choose* μ *large enough so that* $\varepsilon(\mathbf{P_1}, 1)$ *can contain the points* x_{0_k}, *but small enough so that the performance constraints are feasible.*
Step 2: Compute $\mathbf{W_1}, \mathbf{Y_1}, \lambda$ *solutions to:*

$$\min_{\mathbf{W_1},\mathbf{Y_1}} \ \lambda \ \text{ subject to}$$
$$\text{LMIs (19), (20), (21), (22), (23), (24) and (31).}$$

Step 3: Fix $\mathbf{W_1}, \mathbf{Y_1}$. *Compute* $\mu_{(r)},\ r = 1, \ldots, n$ *solution to:*

$$\min \ \sum_{r=1}^{n} \mu_{(r)} \ \text{ subject to } \ \text{LMI (24).}$$

Step 4: Return to Step 1 until the reduction of λ *is not significative.*
Step 5: The controller is recovered by $\mathbf{K} = \mathbf{Y_1}{\mathbf{W_1}}^{-1}$ *and the minimum disturbance rejection for such a controller is given by* λ.
Step 6: With controller $\mathbf{K}$, *choose an initial* μ *large enough so that* $\varepsilon(\mathbf{P_2}, 1)$ *can contain the points* x_{0_k} *and define* u_0.
Step 7: Compute $\mathbf{P_2}$ *solution to:*

$$\min_{\mathbf{P_2}} \ \text{Tr}(\mathbf{P_2}) \ \text{ subject to}$$
$$\text{LMIs (23)}^*, \text{(24)}^* \text{ and (26)}^*. \tag{32}$$

Step 8: Fix $\mathbf{P_2}$. *Compute* $\mu_{(r)},\ r = 1, \ldots, n$ *solution to:*

$$\max \ \sum_{r=1}^{n} \mu_{(r)} \ \text{ subject to } \ \text{LMI (24)}^*. \tag{33}$$

Step 9: Return to Step 7 until the reduction of ($\text{Tr}(\mathbf{P_2})$*) is not large enough.*
Step 10: The region of stability with controller $\mathbf{K}$ *is given by* $\varepsilon(\mathbf{P_2}, 1)$.

Remark IV.1. *Regarding Synthesis Algorithms 2 and 3, in order to deal with the performance requirements and the robustness, the first point that the designer must consider is the uncertainty assumed in the model. If no uncertainty of operating point is considered, matrices* (A_i, B_{u_i}) *with* $N = 1$ *are simply* (A, B_u) *and the stability of trajectories from that nominal operating point can be considered.*

The opposite case can be considered as follows. Usually, each initial condition x_{0_k} *is associated with a plant model* (A_k, B_{u_k}). *If the bilinearity model* (A_k, B_{u_k}) *is also the uncertainty model* (A_i, B_{u_i}), N_k *is equal to* N. *This approach is useful to find a shared region of stability valid for all operating points of the uncertainty model. In that case, the left-hand side of* (23) *can substitute the first block of the left-hand side of* (19). *Obviously, the increase of the number of constraints to be fulfilled can reduce the achievable performance. As an intermediate solution, the designer can consider a set of different operating points and assure the stability of*

Table II
BOOST CONVERTER PARAMETERS

Parameter	Value	Nominal Value
R	[10 , 50] Ω	10 Ω
D'	[0.3 , 1.0]	0.5
v_o (V_{ref})	24 V	–
V_g	12 V	–
C	200 μF	–
L	100 μH	–
T_s	5 μs	–

Table III
POLE PLACEMENT PARAMETERS

Parameter	Value
α	1000
θ	25 deg
ρ	$\frac{2\pi}{10T_s}$

the trajectories for known disturbances at some (but not all) points (A_k, B_{u_k}).

V. DESIGN EXAMPLES

In this section, a synthesis example is presented, in order to illustrate the properties of the proposed synthesis methods. Synthesis algorithms 1, 2 and 3 are applied to the uncertain and nonlinear model of the boost converter shown in Section II, whose parameter set is shown in Table II.

The pole region constraints for parameters $\alpha,\ \rho,\ \theta$ are specified in Table III, following the guidelines of [15]: In order to limit the poles inside the valid frequency range of the averaged model, ρ is set to 1/10 of the switching frequency. For a minimum damping ratio of $\zeta = 0.4$, θ is set to 25 degrees. Finally, the value of α for the required region of stability is equal to 1000, which corresponds to a maximum settling time of 4 ms.

The stability of the converter despite the bilinear term is assured for the nominal operating point $D' = 0.5$. That is, the set of matrices (A_k, B_{u_k}) is given by $(A_k, B_{u_k}) \in \Big[A_1, B_{u_1}(D' = 0.5,\ R = 10), A_2, B_{u_2}(D' = 0.5,\ R = 50)\Big]$. Since the operating point for which the trajectory is assured is $D' = 0.5$ and the duty-cycle is constrained in $d(t) \in [0, 1]$ the maximum control effort in order to avoid the saturation nonlinearity is $u_0 = 0.5$:

$$0 \leq \mathbf{K}X + \mathbf{K}\tilde{x} \leq 1 \leftrightarrow -0.5 \leq \mathbf{K}\tilde{x} \leq 0.5. \qquad (34)$$

Finally, the initial region of the polytopic model of bilinearity, defined by μ is $\mu = [1,\ 1,\ \mu_3]$ unless noted otherwise. As explained in Section II-C, μ_3 does not affect the synthesis results and it must only be kept large enough to not limit the volume of $\varepsilon(\mathbf{P}, 1)$ in the direction of the third state.

A. Synthesis Algorithm 1

For this case, the $\mathcal{H}_\infty$ norm between disturbance and output is limited to $\lambda = 5$. Once all parameters $\alpha,\ \rho,\ \theta,\ \lambda,\ u_0,\ \mu$ are defined, Algorithm 1 yields, after 9 iterations, the following controller vector:

$$K_{nl_1} = [\ -0.11,\ -0.15,\ -266.38]. \qquad (35)$$

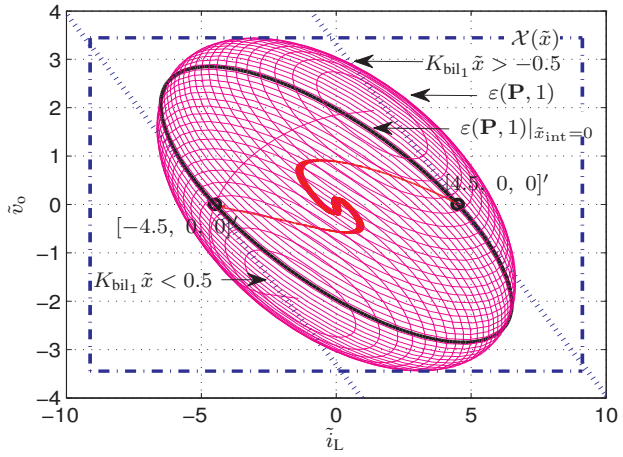

Figure 4. Simulated transient of the trajectories of the boost converter for initial conditions $\pm[4.5,\ 0,\ 0]'$, with controller K_{nl_1}.

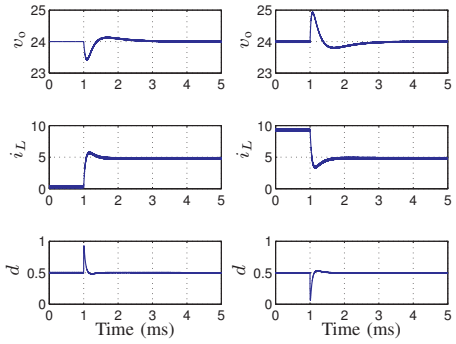

Figure 5. Simulated transient of the boost converter for initial conditions $\pm[4.5,\ 0,\ 0]'$, with controller K_{nl_1}. Left column: $[-4.5,\ 0,\ 0]'$; Right column:$[+4.5,\ 0,\ 0]'$. Top waveforms: output voltage; middle waveforms: inductor current; bottom waveforms: duty-cycle.

and a resulting λ equal to 3.02 (9.6 dB). The region of stability $\varepsilon(\mathbf{P}, 1)$ assured with this controller can be observed in Fig. 4. The figure shows the ellipsoid of attraction $\varepsilon(\mathbf{P}, 1)$ and its section on the plane $(\tilde{i}_L,\ \tilde{v}_o)$ for $\tilde{x}_{int}$ equal to zero. It can be observed that this ellipsoid is included in the polyhedral set $\mathcal{X}(\tilde{x})$. The trajectories of the converter states for two different initial conditions at two extremes of the ellipsoid ±[4.5, 0, 0]' are also depicted. The simulations are carried out with the switched-mode circuit of Fig. 1 using PSIM [27]. The trajectories and control effort waveforms can also be observed in the time-domain in Fig. 5, for the same initial conditions in the inductor current of ±4.5 A. The upper waveform of the figure shows the output voltage signal v_o, while the waveform in the middle depicts the inductor current i_L. Note that the control effort remains in the specified region $d(t) \in [0, 1]$ and the settling time, damping ratio and disturbance rejection requirements are also satisfied.

B. Synthesis Algorithm 2

For the third algorithm, the trade-off between performance and stability is treated as follows. The uncertainty description considers that the load R belongs to the set $[10,\ 50]\ \Omega$. In order to guarantee the stability when switching between

Table IV
SPECIFIC INITIAL CONDITIONS

x_{0_k}	Value	(A_k, B_{u_k})
x_{0_1}	$\pm[3.84,\ 0,\ x_{\text{int}_0}]$	$A_1, B_{u_1} (D' = 0.5,\ R = 10\ \Omega)$
x_{0_2}	$\pm[3.84,\ 0,\ x_{\text{int}_0}]$	$A_2, B_{u_2} (D' = 0.5,\ R = 50\ \Omega)$

the maximum and the minimum load at a certain operation point, such specific initial conditions x_0 are included in the ellipsoidal region of stability. Since the nominal duty-cycle is $D' = 0.5$, the inductor current drops from 4.8 A to 0.96 A when the load switches between 10 Ω and 50 Ω, which corresponds to a current step of ±3.84 A. Assuming that the converter is in steady-state before the load change, x_0 is then equal to $\pm[3.84,\ 0,\ x_{\text{int}_0}]$ (Table IV).

Note that, in the previous paragraph, the point x_0 has not been completely defined. The value of x_{int_0} depends on the control gain $\mathbf{K}$, and therefore, it can not be specified a priori. The following procedure is proposed: x_{int_0} is set to zero at the first iteration of the synthesis algorithm. Then, x_0 is updated to contain $x_{\text{int}_0} = (-3.84K_1)/K_3$ at each new iteration. This approach assures that the trajectory of the converter states will be bounded in the region of stability. Since $\varepsilon(\mathbf{P}, 1)$ must contain the points x_0, the initial state vector μ is enlarged up to $\mu = [8,\ 4,\ \mu_3]'$.

Once defined $\alpha,\ \rho,\ \theta,\ u_0,\ \mu$ and x_0, Algorithm 2 yields, after 3 iterations, the following gain vector

$$K_{\text{nl}_2} = [\ -0.14,\ -0.23,\ -363.74]. \tag{36}$$

This controller assures a minimum $\mathcal{H}_\infty$ performance factor of $\lambda_{\text{bil}} = 2.45$ (7.78 dB). The final values of μ and x_0 are $[5.97,\ 2.94,\ \mu_3]$ and $[3.84,\ 0,\ 1.47 \cdot 10^{-3}]$ respectively. The resulting region of stability is depicted in Fig. 6, where the resulting trajectories for the initial conditions $\pm x_0$ are also shown. As expected, the trajectories of the system remain inside the region of attraction and converge to the equilibrium point. The inclusion of the integrator state x_{int} in the synthesis algorithm allows to simulate the change of operating points as load switchings. The time-domain response to such load variations is shown in Fig. 7. As it can be observed in the output current waveform of the figure, the converter load is initially the minimum value ($R = 50\ \Omega$). At $t = 1$ ms, the load changes to its maximum value ($R = 10\ \Omega$) and at $t = 6$ ms, it returns to its original value. As expected, it can be observed that the performance requirements are satisfied, since the settling time is approximately 2 ms and the damping ratio is larger than 0.4. It can also be noted that Algorithm 2 allows to obtain better disturbance rejection than Algorithm 1. However, it may be difficult to obtain a unique Lyapunov function $\mathbf{P}$ that satisfies all constraints at the same time. Algorithm 3 relaxes such limitations and allows to improve the performance of the resulting synthesized controller.

C. Synthesis Algorithm 3

Considering the same set of initial conditions x_0 and a control effort constraint of $u_0 = 0.5$, Algorithm 3 yields, after 12 iterations, the gain vector

$$K_{\text{nl}_3} = [\ -0.36,\ -1.07,\ -1922.87]. \tag{37}$$

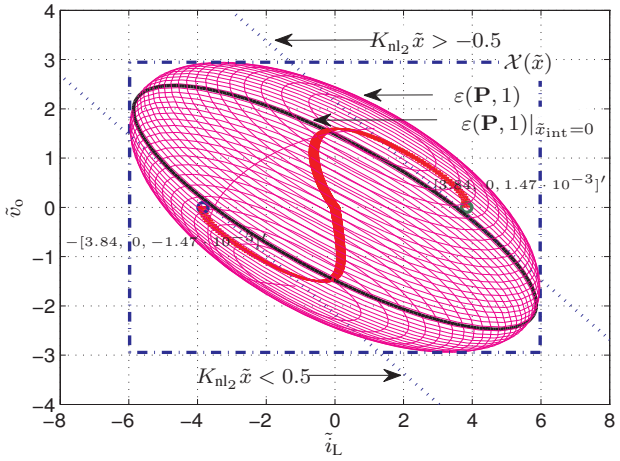

Figure 6. Simulated transient of the trajectories of the boost converter with controller K_{nl_2} for load switchings between 10 Ω and 50 Ω.

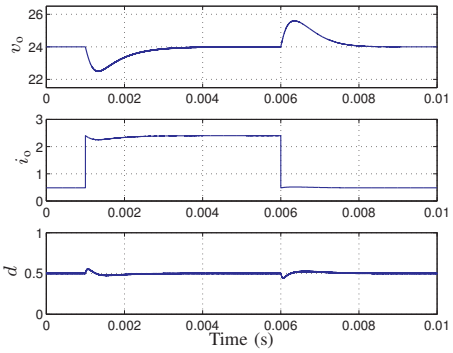

Figure 7. Simulated transient of the boost converter under a load step transient equivalent to initial conditions $\pm[3.84,\ 0,\ 1.47 \cdot 10^{-3}]'$ with controller K_{nl_2}. Top waveforms: output voltage; middle waveforms: inductor current; bottom waveforms: duty-cycle.

The $\mathcal{H}_\infty$ disturbance rejection ratio is $\lambda_{\text{bil}} = 1.69$ (4.55 dB), while μ and x_0 are $[7.16,\ 2.05,\ \mu_3]$ and $[3.84,\ 0,\ 0.72 \cdot 10^{-3}]$ respectively. Besides, this approach allows to increase settling time specification up to α=1600. Figs. 8 and 9 show the region of stability and the transient numerical simulations for the same load step changes of the previous section. Fig. 8 shows the regions of stability $\varepsilon(\mathbf{P_1}, 1)$ and $\varepsilon(\mathbf{P_2}, 1)$. While $\varepsilon(\mathbf{P_1}, 1)$ does not fulfill the control effort constraint, $\varepsilon(\mathbf{P_2}, 1)$ fulfills this constraint and also contains the initial conditions x_0. The numerical simulation of Fig. 9 illustrates the performance improvement that can be achieved with Synthesis Algorithm 3 with respect to Synthesis Algorithm 2. The output voltage deviation is approximately one half of the deviation observed in Fig. 7, while, at the same time, the control effort remains in the allowed region.

D. Comparison with previous results

Since Synthesis Algorithm 3 provides the best trade-off between performance and stability, we have compared it with the previous results of [15]. A controller, noted K_{lin}, has been synthesized using the controller synthesis method proposed in [13], with the objective to compare the performance and robustness characteristics.

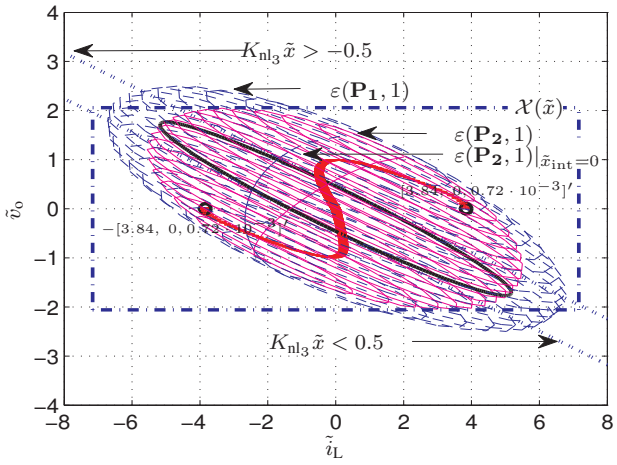

Figure 8. Simulated transient of the trajectories of the boost converter with controller K_{nl_3} for load switchings between 10 Ω and 50 Ω.

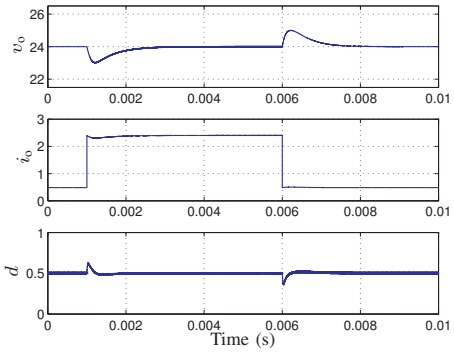

Figure 9. Simulated transient of the boost converter under a load step transient equivalent to initial conditions $\pm[3.84,\ 0,\ 0.72\cdot 10^{-3}]'$ with controller K_{nl_3}. Top waveforms: output voltage; middle waveforms: inductor current; bottom waveforms: duty-cycle.

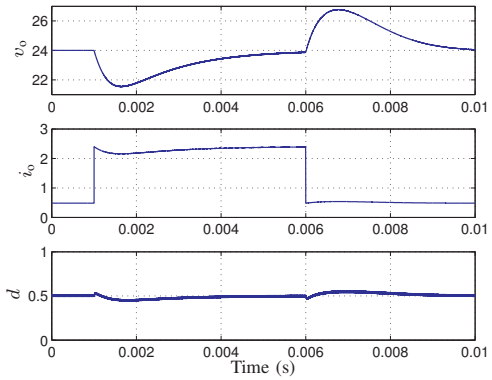

Figure 10. Simulated transient of the boost converter under a load step transient equivalent to initial conditions $\pm[+3.84,\ 0,\ 0.72\cdot 10^{-3}]'$ with controller K_{lin}. Top waveforms: output voltage; middle waveforms: inductor current; bottom waveforms: duty-cycle.

Controller K_{lin} has been synthesized with the uncertainty model proposed in the mentioned work, and the achieved performance factor is $\lambda_{\mathrm{lin1}} = 4.81$ (13.64 dB). The same transient simulation of Fig. 9 has been carried out with the linear controller and the results have been depicted in Fig. 10. It can be pointed out that with the proposed synthesis method, the output voltage presents a deviation of approximately 1 V

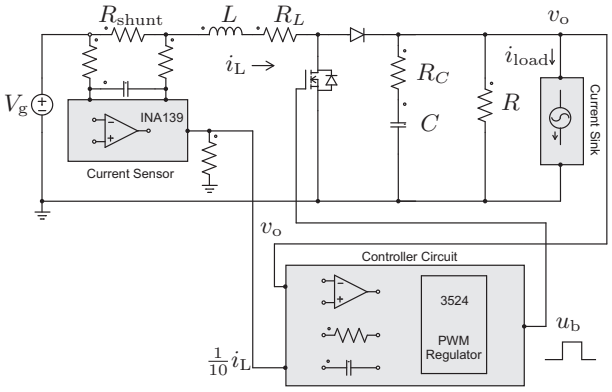

Figure 11. Implementation diagram of a boost converter with state-feedback regulation.

($\lambda = 0.57$, -4.83 dB) while with controller K_{lin} the deviation is approximately 2 times larger ($\lambda = 1.30$, 2.29 dB). Besides, the settling time after each disturbance is approximately 4 times smaller with the proposed approach. In addition, with the control synthesis method of [13] the control effort was not guaranteed to be inside the nonsaturated region and that the trajectory was stable despite the bilinear dynamics. Thus, the proposed approach allows to obtain better performances while maintaining the desired robustness properties.

VI. Control Implementation and Experimental Results

In order to verify the results derived in the previous sections, a 100 W boost converter has been built. The structure of the converter with the proposed controller can be seen in Fig. 11, where the component values are those in Table II. A shunt resistance of $R_{shunt} = 25$ mΩ and an INA139 differential amplifier have been used to measure the inductor current. The load change experiments have been carried out by means of a voltage-controlled switch. A detail of controller K_{nl_3} is given in Fig. 12. Note that the proposed implementation requires two additional operational amplifiers with respect to the circuits shown in [14], [15], which can be used to set the initial conditions of the reference and the integrator.

Fig. 13 shows the transient waveforms of the converter with controller K_{nl_3} under the load perturbation simulated in the previous section. It can be observed a perfect agreement with respect to the simulation results of Fig. 9.

Finally, the inductor current/output voltage of the converter under the same load changes are verified. By comparing Fig. 8 with Fig. 14, it can be concluded that the experimental results and numerical simulations are in good agreement.

VII. Conclusions

This paper proposes a robust controller synthesis method for bilinear dc-dc converters. The method allows to specify beforehand the common requirements of such power devices, to deal with the uncertainty of their components and to consider their nonlinearities. A minimum level of transient and steady-state performances can be assured, as the $\mathcal{H}_\infty$ norm between a disturbance and the output, and the decay

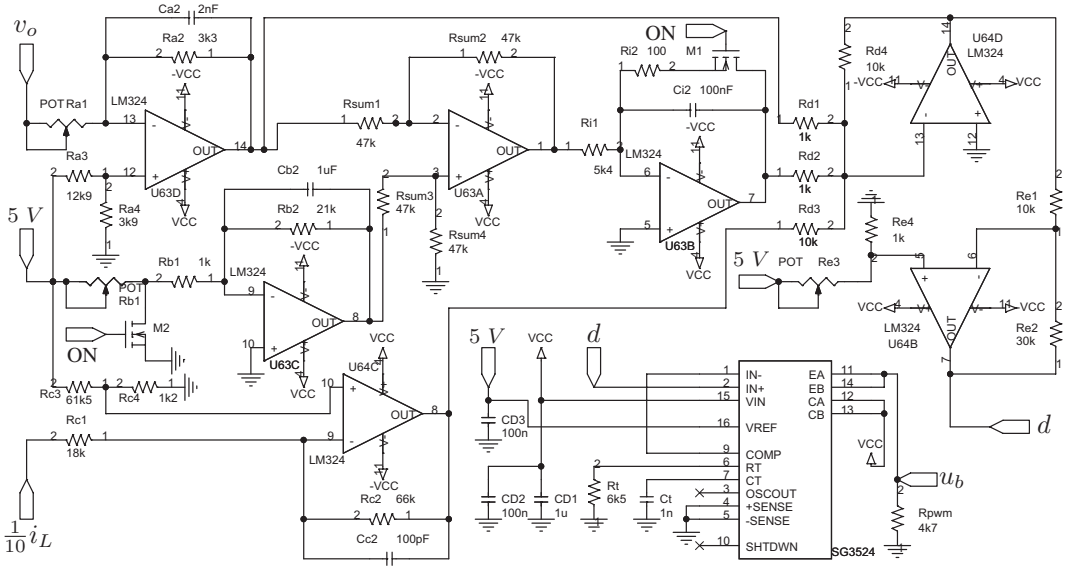

Figure 12. Detail of the circuit implementation of the robust controller K_{nl_3} with the PWM regulator.

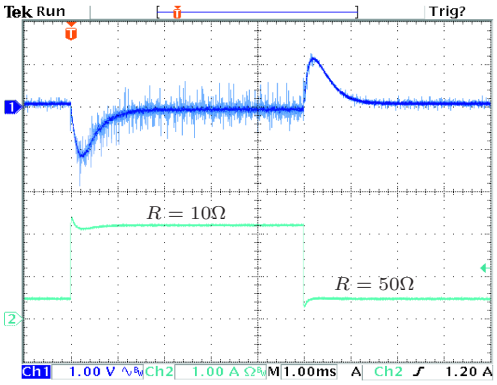

Figure 13. Experimental transient of the boost converter under a load step transient of 1.92 A at nominal duty-cycle $D'_d = 0.5$ with the proposed controller K_{nl_3}. Upper traces are output voltage. Lower traces are output current.

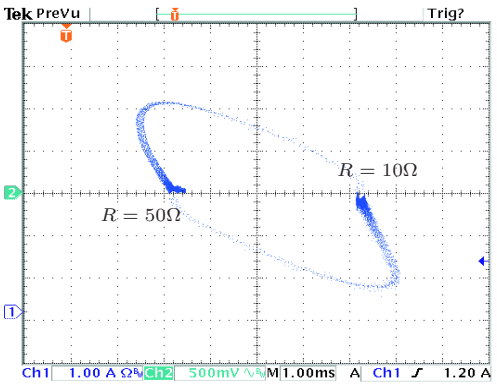

Figure 14. Experimental trajectories of the boost converter under a load step transient of 1.92 A at nominal duty-cycle $D'_d = 0.5$ with the proposed controller K_{nl_3}. Channel 1 is inductor current i_{L}. Channel 2 is output voltage.

rate and overshoot of the regulation. The uncertainty of the load and the changes of operating point (equivalent to the uncertainty of the input voltage) have been taken into account. The bilinear dynamics of the converter have been included in a convex model, in order to assure the stability of the closed-loop system in a region defined by an ellipsoid, which is an approximation of the real region of stability. Besides, the saturation nonlinearity has been avoided with other constraints that verify that the control effort for specific operating point changes is kept inside the linear region. The combination of these constraints has resulted in several synthesis algorithms, which have been discussed and compared. The numerical simulations, and more importantly, the experimental results, have verified the theoretical basis of the proposed methods.

Future works will deal with improvements in the uncertainty modeling, in order to consider, for example, nonresistive loads or other parametric changes. Another important requirement in dc-dc converters is the capability to maintain the robustness and performance characteristics during startup, hence the derivative of the voltage reference could be treated in other investigations. It is worth to point out that our approach considers a unique quadratic Lyapunov function that must satisfy all the requirements. Thus, in order to improve the synthesis results, other investigations could deal with the inclusion of parameter-dependent Lyapunov functions that may result in more accurate approximations of the region of stability. Also, the LMI procedure could be applied to exact discrete time models which are able to cope with fast scale instabilities that eventually lead to subharmonic oscillations and chaotic behavior. Such a fast scale instability usually takes place when there is an excess of ripple component at the switching frequency, as reported in [28]. Finally, the approach used here can be extended to other more complex converters such as parallel converters, multi-level converters, AC-DC power factor correction circuits and DC-AC inverters.

ACKNOWLEDGMENT

This work was partially supported by the Spanish *Ministerio de Educación y Ciencia* under grant *Estancias de Movilidad Postdoctoral, EX2009-0011*.

REFERENCES

[1] R. W. Erickson and D. Maksimovic, *Fundamentals of Power Electronics*. Norwell, Massachusetts: Kluwer Academic, 1999.

[2] F. M. Oettmeier, J. Neely, S. Pekarek, R. DeCarlo, and K. Uthaichana, "Mpc of switching in a boost converter using a hybrid state model with a sliding mode observer," *IEEE Transactions on Industrial Electronics*, vol. 56, no. 9, pp. 3453–3466, 2009.

[3] A. G. Perry, F. Guang, L. Yan-Fei, and P. C. Sen, "A design method for pi-like fuzzy logic controllers for DC-DC converter," *IEEE Transactions on Industrial Electronics*, vol. 54, no. 5, pp. 2688–2696, 2007.

[4] G. Liping, J. Y. Hung, and R. M. Nelms, "Evaluation of DSP-based PID and fuzzy controllers for DC-DC converters," *IEEE Transactions on Industrial Electronics*, vol. 56, no. 6, pp. 2237–2248, 2009.

[5] A. M. Rahimi and A. Emadi, "Active damping in DC-DC power electronic converters: A novel method to overcome the problems of constant power loads," *IEEE Transactions on Industrial Electronics*, vol. 56, no. 5, pp. 1428–1439, 2009.

[6] A. G. Beccuti, S. Mariethoz, S. Cliquennois, W. Shu, and M. Morari, "Explicit model predictive control of DC-DC switched-mode power supplies with extended Kalman filtering," *IEEE Transactions on Industrial Electronics*, vol. 56, no. 6, pp. 1864–1874, 2009.

[7] H. El Fadil and F. Giri, "Robust nonlinear adaptive control of multiphase synchronous buck power converters," *Control Engineering Practice*, vol. 17, no. 11, pp. 1245–1254, 2009.

[8] H. El Fadil, F. Giri, O. El Magueri, and F. Z. Chaoui, "Control of dc-dc power converters in the presence of coil magnetic saturation," *Control Engineering Practice*, vol. 17, no. 7, pp. 849–862, 2009.

[9] R. Cardim, M. C. M. Teixeira, E. Assuncao, and M. R. Covacic, "Variable-structure control design of switched systems with an application to a DC-DC power converter," *IEEE Transactions on Industrial Electronics*, vol. 56, no. 9, pp. 3505–3513, 2009.

[10] V. F. Montagner, R. C. L. Oliveira, P. L. D. Peres, S. Tarbouriech, and I. Queinnec, "Gain-scheduled controllers for linear parameter-varying systems with saturating actuators: LMI-based design," in *Proceedings of the American Control Conference, ACC '07*, 2007, pp. 6067–6072.

[11] C. A. Torres-Pinzon and R. Leyva, "Fuzzy control in DC-DC converters: an LMI approach," in *Proceedings of the IEEE Annual Conference on Industrial Electronics, IECON'09*, Porto, 2009, pp. 510–515.

[12] E. Vidal-Idiarte, L. Martinez-Salamero, J. Calvente, and A. Romero, "An H_∞ control strategy for switching converters in sliding-mode current control," *IEEE Transactions on Power Electronics*, vol. 21, no. 2, pp. 553–556, 2006.

[13] C. Olalla, R. Leyva, A. El Aroudi, and P. Garcés, "QFT robust control of current-mode converters: application to power conditioning regulators," *International Journal of Electronics*, vol. 96, no. 5, pp. 503–520, 2009.

[14] C. Olalla, R. Leyva, A. El Aroudi, and I. Queinnec, "Robust LQR control for PWM converters: an LMI approach," *IEEE Transactions on Industrial Electronics*, vol. 56, no. 7, pp. 2548–2558, 2009.

[15] ——, "LMI robust control design for boost PWM converters," *IET Power Electronics*, vol. 3, no. 1, pp. 75–85, 2010.

[16] M. Chilali and P. Gahinet, "H$_\infty$ design with pole placement constraints: an LMI approach," *IEEE Transactions on Automatic Control*, vol. 41, no. 3, pp. 358–367, 1996.

[17] G. Garcia, J. Daafouz, and J. Bernussou, "Output feedback disk pole assignment for systems with positive real uncertainty," *IEEE Transactions on Automatic Control*, vol. 41, no. 9, pp. 1385–1391, 1996.

[18] S. Tarbouriech, G. Garcia, and A. H. Glattfelder, *Advanced strategies in control systems with input and output constraints*, ser. Lecture Notes in Control and Information Sciences, vol. 346. Berlin: Springer, 2007.

[19] S. Boyd, L. El Ghaoui, E. Feron, and V. Balakrishnan, *Linear Matrix lnequalities in Systems and Control Theory*, ser. Studies in Applied and Numerical Mathematics. Philadelphia: SIAM, 1994, vol. 15.

[20] P. Gahinet, A. Nemirovski, A. J. Laub, and M. Chilali, *LMI Control Toolbox for use with Matlab*. The MathWorks, Inc., 1995.

[21] R. T. Rockafellar, "Lagrange multipliers and optimality," *SIAM Review*, vol. 35, no. 2, pp. 183–238, 1993.

[22] R. Leyva, A. Cid-Pastor, C. Alonso, I. Queinnec, S. Tarbouriech, and L. Martinez-Salamero, "Passivity-based integral control of a boost converter for large-signal stability," *IEE Proceedings Control Theory and Applications*, vol. 153, no. 2, pp. 139–146, 2006.

[23] N. J. Krikelis and S. K. Barkas, "Design of tracking systems subject to actuator saturation and integrator wind-up," *International Journal of Control*, vol. 39, no. 4, pp. 667–682, 1984.

[24] J. M. Biannic, C. Roos, and A. Knauf, "Design and robustness analysis of fighter aircraft flight control laws," *European Journal of Control*, vol. 12, no. 1, pp. 71–85, 2006.

[25] S. Tarbouriech, I. Queinnec, T. R. Calliero, and P. L. D. Peres, "Control design for bilinear systems with a guaranteed region of stability: An LMI-based approach," in *17th Mediterranean Conference on Control and Automation*, Thessaloniki, 2009, pp. 809–814.

[26] P. Gahinet and P. Apkarian, "A linear matrix inequality approach to H_∞ control," *International Journal of Robust and Nonlinear Control*, vol. 4, no. 4, pp. 421–448, 1994.

[27] POWERSIM, "PSIM 6.0," 2003, [Online] `http://www.powersimtech.com`.

[28] A. El Aroudi, E. Rodriguez, R. Leyva, and E. Alarcon, "A design-oriented combined approach for bifurcation prediction in switched-mode power converters," *IEEE Transactions on Circuits and Systems II: Express Briefs*, vol. 57, no. 3, pp. 218–222, 2010.

Carlos Olalla (M'06) obtained the graduate degree in electronics engineering from Universitat Rovira i Virgili, Tarragona, Spain, in 2004, and the Ph.D degree in advanced automatic control from Universitat Politècnica de Catalunya, Barcelona, Spain, in 2009, for his work on robust linear control of power converters, during his stay in the GAEI research group of Universitat Rovira i Virgili. He was a visiting scholar at the *Laboratoire d'Analyse et d'Architecture des Systèmes* (LAAS-CNRS), Toulouse, France, in 2007 and 2009, and he held a 6 month postdoctoral position during 2009 and 2010, where he continued his research in modelling of power converters and robust control theory. He is currently a visiting scholar in the Colorado Power Electronics Center (CoPEC), Dept. of Electrical, Computer, and Energy Engineering, University of Colorado, Boulder CO, USA, where he works on control synthesis methods for digitally controlled power converters.

Isabelle Queinnec is currently CNRS researcher at LAAS-CNRS, Université de Toulouse. She received her PhD degree and HDR degree in automatic control in 1990 and 2000, respectively, from University Paul Sabatier, Toulouse. Her current research interests include constrained control and robust control of processes, with particular interest in applications on aeronautical systems, biochemical and environmental processes. She serves as member of the IFAC technical committees on "Biosystems and Bioprocesses" and on "Modelling and Control of Environmental Systems", respectively from 2002 and 2005.

Ramon Leyva (M'01) received Telecommucation Engineering and Ph.D. degrees from Universitat Politècnica de Catalunya, Barcelona, Spain, in 1992, and 2000, respectively. He is currently an Associate professor with the Departament d'Enginyeria en Electrònica, Elèctrica i Automàtica, Universitat Rovira i Virgili, Tarragona, Spain. From March 2002 to March 2003, he was holding a visiting scholarship at the Laboratoire d'Analyse et d'Architecture des Systèmes (LAAS-CNRS), Université de Toulouse, France. He is reviewer for several IEEE and IET scientific publications. His research task is being developed in the field of nonlinear and robust control of power switching converters.

Abdelali El Aroudi (M'00) was born in Tangier (Morocco), in 1973. He obtained the graduate degree in physical science from Faculté des sciences, Université Abdelmalek Essadi, Tetouan, Morocco, in 1995, and the Ph.D degree (with honors) from Universitat Politècnica de Catalunya, Barcelona, Spain in 2000. During the period 1999-2001 he was a visiting Professor at the Department of Electronics, Electrical Engineering and Automatic Control, Technical School of Universitat Rovira i Virgili (URV), Tarragona, Spain, where he became an associate professor in 2001 and a full-time tenure Associate Professor in 2005. During the period September 07-January 08 he was holding a visiting scholarship at the Department of Mathematics and Statistics, National University of Colombia, Manizales, conducting research on modeling of power Electronics circuits for energy management. From February 2008 to July 2008, he was a visiting scholar at the *Centre de Recherche en Sciences et Technologies de Communications et de l'Informations* (CReSTIC), Reims, France. He has participated in three Spanish national research projects and five cooperative international projects. His research interests are in the field of structure and control of power conditioning systems for autonomous systems, power factor correction, stability problems, nonlinear phenomena, chaotic dynamics, bifurcations and control. He is a reviewer for *IEEE Transaction on Circuits and Systems part. I- Regular papers and II Express Briefs, IEEE Transactions on Power Electronics, IEEE Transactions on Industrial Electronics, International Journal of Control, International Journal of Power Electronics, IET Electric Power Applications, International Journal of Systems Science, Circuits, Systems and Signal Processing*, *International Journal of Sound and Vibration* and *Nonlinear Dynamics*. He has published about 90 papers in scientific journals and conference proceedings. He is a member of the GAEI research group (Rovira i Virgili University) on Industrial Electronics and Automatic Control whose main research fields are power conditioning for vehicles, satellites and renewable energy. He has given invited talks in several universities in Europe, South America and Africa.